

# Performance Characteristics between Horizontally and Vertically Oriented Electrodes EHD-ESP for Collection of Low-Resistive Diesel Particulates

Toshiaki Yamamoto

Fellow, IEEE  
Tokyo City University  
Setagaya-ku, Tokyo,  
158-8557 Japan  
yama-t@tcu.ac.jp

Takahisa Sakurai

Tokyo City University  
Setagaya-ku, Tokyo,  
158-8557 Japan  
G1081332@tcu.ac.jp

Yoshiyasu Ehara

Tokyo City University  
Setagaya-ku, Tokyo, 158-8557 Japan  
yehara@tcu.ac.jp

Akinori Zukeran

Kanagawa Institute of Technology  
Atsugi, Kanagawa,  
243-0292 Japan  
zukeran-akinori@ele.kanagawa-it.ac.jp

Hitomi Kawakami

Fuji Electric Co. Ltd.  
Tokyo, 191-8502, Japan  
Kawakami-hitomi@fujielectric.co.jp

**Abstract** -- The novel electrohydrodynamically-assisted electrostatic precipitator (EHD ESP) was developed to suppress particle reentrainment for collection of low resistive diesel particulates. The collection efficiency was compared between vertically and horizontally oriented electrodes of the EHD ESP using 400 cc diesel engine. The particle size dependent collection efficiency was evaluated for the particle size ranging in 20 to 5,000 nm using a scanning mobility particle sizer (SMPS) and a particle counter (PC). Both horizontally and vertically oriented EHD ESP showed an excellent suppression of particle reentrainment. However, the horizontally oriented electrode EHD ESP showed significantly improved for the particle size of 300-500 nm in comparison with vertically oriented electrode EHD ESP, resulting in more than 90% collection efficiency for all particle size range. The EHD ESP has high potential especially for highly concentrated marine diesel engine emission control.

**Index Terms**—diesel engine, diesel emission control, particulates, marine emission, electrostatic precipitator, electrohydrodynamics, reentrainment, air pollution control

## I. INTRODUCTION

The particles emitted from diesel engine exhaust are low resistive in nature and extremely small in the range of 70~120 nanometers (nm). These particles are penetrated into an alveolus and extremely harmful to human health. These particles are generated from various emission sources such as diesel automobiles, marine engines, power generation engines, and construction machines. The collection of low resistive particles (PM) has been known to be extremely difficult. The low resistive diesel engine particles are detached from the collection plate where the electrostatic repulsion force due to induction charge exceeds particle adhesion force on the collection electrode. This phenomenon has been known as particle reentrainment or resuspension, resulting in poor collection efficiency. The use of diesel particulate filter (DPF) was widely used for the collection of automobile diesel PM but was not economical and cost effective, especially for marine engine emission where PM concentration is often exceed 100 mg/m<sup>3</sup>.

The regulation for 3.5 tons automobile diesel particulate matter (PM) emission was 0.7 g/kWh in year 2009. On the

other hand, the marine engine PM regulation was not strictly set by MARPOL treaty in 2005. However, PM emission from the ship damaged the exporting new cars during shipment. More stringent regulations are forced by TEER-3 by 2011 and TEER-4 by 2016 (80% of NO<sub>x</sub> reduction at the present level).

There are few literatures describing the control of particle reentrainment [1-3]. Recently, two-stage ESP i.e., charging field using DC field, followed by the collection field using low frequency AC field including the trapezoidal waveforms in the range of 1-20 Hz has been investigated for the collection of diesel particles in tunnel [4-6], while the conventional ESP utilizes DC high voltage. Several particle trapping design collection plates were reported but were not taken into account the electrohydrodynamics (EHD) to transport the charged particles into the pocket zone [7]. Some ESP manufactures use the corrugated collection plates. However, the primary reason was to increase the strength of large and long ESP collection plates. This design may help preventing trapping loss in the corrugated section but both concepts have limited success for minimizing the reentrainment. Recently, electrostatic flocking filter on the collection electrode was developed to capture fine diesel particles [12]. The wet ESP was another strong candidate for this application but it creates water treatment as opposed to dry process.

Based on fundamentals of reentrainment theory, the new electrohydrodynamically-assisted ESP (EHD ESP) was developed to overcome the reentrainment in the ESP [8-10]. The EHD ESP, which utilizes the ionic wind to transport the charged particles effectively into the zero or low electrostatic field zone (or pocket zone) attached to the collection plate. The captured particles are trapped in the pocket and the particle captured in the pocket zone was exposed to zero electric field, so that no electrostatic repulsion force by induction charge takes place, which is the major contribution for the reduction of particle reentrainment. Obviously, the particle exposed to electrostatic field experiences the electrostatic repulsion force. The effectiveness of the EHD

ESP was demonstrated to show the significant suppression of particle reentrainment [8-9]. In the previous report, the electrode was vertically oriented to assure the definite corona discharge or ionic wind on both collection plates. However, the pressure drop was higher and gas velocity became also higher for vertically oriented electrode of the EHD ESP. The horizontally oriented electrode was set and the collection efficiency was compared between vertically and horizontally oriented electrodes of the EHD ESP. The particle size-dependent collection efficiency was obtained using Scanning Mobility Particle Sizer (SMPS TSI) with particle size in the range of 20-500 nm and particle counters (RION PC) with particle size in the range of 300-5,000 nm. The effectiveness of reentrainment or collection efficiency for vertically and horizontally oriented electrodes EHD ESPs was compared. The engine size used were 199 and 435cc using light oil, which the maximum gas velocity obtained in the EHD ESP was 0.34 m/s for 199cc engine and 0.74 m/s for 435cc engine and the applied voltages were set at -12 kV, respectively.

## II. EXPERIMENTAL SETUP

Emissions from a small diesel engine generator (Yammer Co., Ltd., YDG200A-5E, direct injection type for a single cylinder, displacement volume of 199cc, maximum electric power output of 1.7 kW) and 435cc diesel engine (Yammer Co., Ltd., YDG500VS-5E) using light oil were used. The constituents of the diesel PM investigated were 99% of C, 0.1% of Si, 0.07% of Fe, 0.1% of Ca, 0.4% of S, and 0.03% of Zn. In order to determine the number particle density in the ESP, the flue gas was diluted approximately 1,000 times by ambient air and particle size-dependent number densities before and after the ESPs were determined by the SMPS (Scanning Mobility Particle Sizer, Model 3034) for the particle size ranged 20-800 nm and the particle counter (Rion KC-01C) for the particle size of 300-5,000 nm, respectively. The exhaust gas temperature was nearly 20°C. The gas velocity was measured by the hot wire anemometer (Kanomax)

The vertically and horizontally oriented EHD ESPs used for this experiment were shown in Figs. 1 and 2 and their dimensions were designated in the figures. The EHD ESP consists of five teeth shaped electrodes and the collection plate with six pockets. The channel width was 60 mm and its effective height was 200 mm. The 10 mm deep and 20 mm long pocket are attached to the collection plate with every 60 mm interval as shown in Fig. 2, while the conventional ESP was the exactly the same as the EHD ESP without pockets. The EHD ESP reported earlier [8] was modified to add several 2 mm diameter holes every 10 mm spacing on the backside of the pockets in the ESP as indicated in Figs. 1 and 2 in order to minimize the reentrainment due to recirculation generated inside of the pockets and also to minimize the pressure drop within the EHD ESP. The discharge electrode was the saw type, and their teeth were equally spaced with the interval of 10 mm. The distance between the discharge electrode and the upstream backside of the pocket was maintained at 20 mm for the vertically oriented electrodes, while the horizontally oriented electrode was placed 20 mm

from the tip of saw electrode to the upstream side of backside pocket. The overall dimension of ESP section was 300 mm high and 420 mm wide without hopper and inlet and outlet transitions. The flue gas was connected to inlet and outlet of the ESP through the transition where 50% opening perforated plates were placed to achieve a uniform flow in the ESP. The bottom section of the EHD ESP has hopper section with buffer plates, so that particle sneaking was minimized. The top section can be replaced with plexiglass for visualizing EHD flows and particle transport phenomena in the EHD ESP. Fig. 3 shows the schematic diagram of the experimental setup for the conventional and EHD ESP performance evaluation.

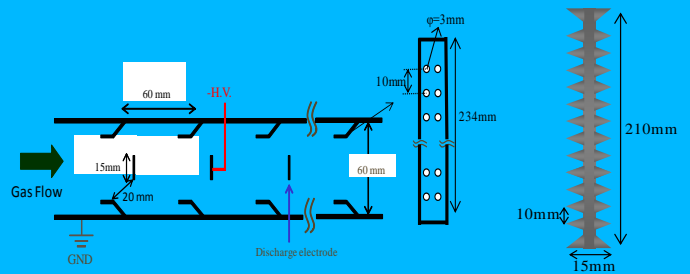


Fig. 1. The vertically oriented electrode EHD ESP configuration

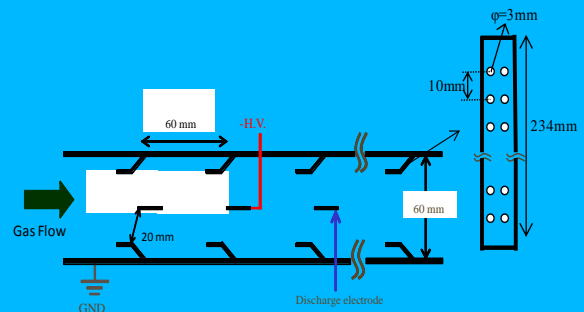


Fig. 2. Horizontally oriented electrode EHD ESP configuration

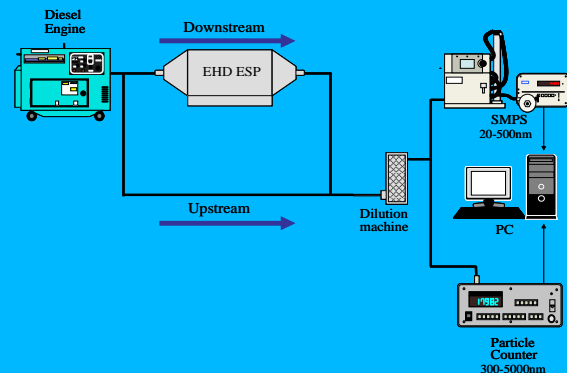


Fig. 3. Schematic diagram of the experimental setup for the conventional and EHD ESP performance evaluation

### III. RESULTS AND DISCUSSION

Experiments were performed using 435cc diesel engine with light oil. When the engine load was set at 70% (3.0 kW) with the gas flow velocity of 0.76 m/s, the particle-size dependent number density in the range of 20~5000 nm was evaluated using SMPS (20~500 nm) and PC (300~5000 nm) for the conventional ESP and vertically and horizontally oriented EHD ESP. Fig. 4 shows the particle-size dependent collection efficiency for particle size of 20~500 nm measured by the SMPS and time-dependent collection efficiency for 300~5000nm measured by the PC for the conventional ESP without pocket and the EHD ESP when the applied DC voltage was set at  $V=-12$  kV although the spark voltage was 18kV (6 kV/cm based on the shortest distance of 20 mm). The collection efficiency for the EHD ESP is slightly better than the conventional ESP. However, the severe particle reentrainment was observed for the particle size of 2000-5000 in the conventional ESP, while particle reentrainment was suppressed for the EHD ESP, which was basically attributed to reduced particle repulsion force due to induction charge for large particles, while adhesion force was dominated for the small particle size.

The adhesion force,  $F_{ad}$  (N) was Van der Waals force, expressed as:  $F_{ad} = -Hd/12z^2$ , where  $H$  = Hamaker constant ( $21.4 \times 10^{-20}$  J),  $d$  = particle diameter (m), and  $z$  = particle separation (m).  $F_{ad}$  consists of adhesion force which depends on the area of contact zone and capillary force when the moisture exists between particle and surface. An empirical adhesion force (dyn or  $10^{-5}$  N) for spherical aluminum oxide particle of 10~50  $\mu\text{m}$  in diameter to a steel surface give the following equation [9]:  $F_{ad} = 2.6d^{-0.7}$  for  $d=10\sim 50\mu\text{m}$ . The adhesion force dominated over the electrostatic repulsion force due to induction charge for the particle size in the range of 20~300 nm, which results in no reentrainment even for the conventional ESPs.

Fig. 4 shows the particle size dependent collection efficiency for the conventional ESP and EHD ESP for particle size of 20~500nm measured by the SMPS using 199cc diesel engine with the engine load of 25%. The collection efficiency exceeded more than 90% for all particle size range measured but the collection efficiency for the EHD ESP showed better

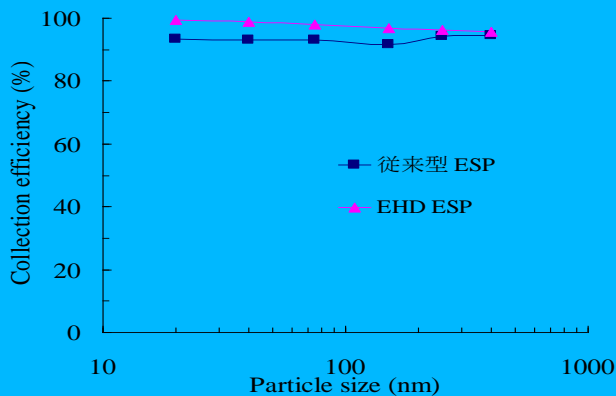


Fig. 4. Particle-size dependent collection efficiency for the conventional ESP and the EHD ESP for particle size of 20~500 nm measured by the SMPS using 199cc diesel engine

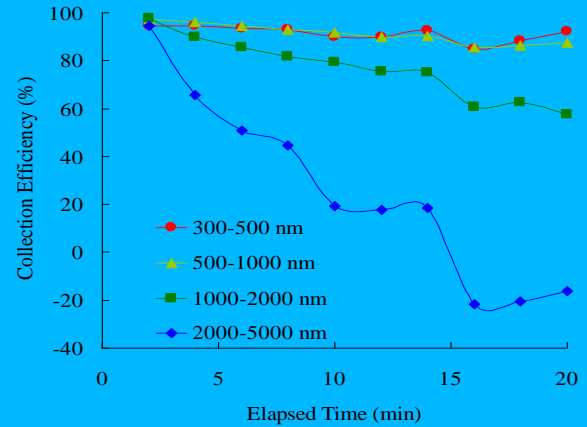


Fig. 5(a) Time-dependent collection efficiency as a function of particle size of 300~5000 nm measured by the PC for the conventional ESP for particle size using 199cc engine

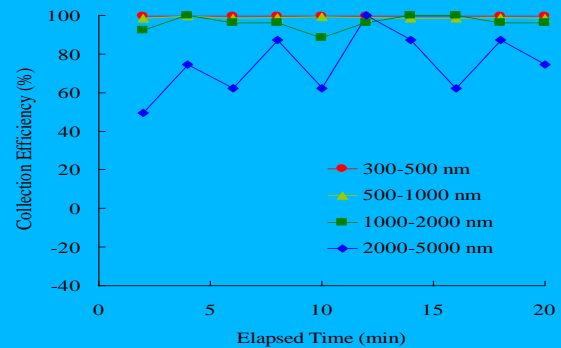


Fig. 5(b) Time-dependent collection efficiency as a function of particle size of 300~5000 nm measured by the PC for the EHD ESP using 199cc diesel engine

efficiency, especially for the particle size of less than 200 nm by approximately 5%. The time-dependent collection efficiency as a function of particle size of 300~5000 nm measured by the PC for the conventional ESP as shown in Fig. 5(a) and the EHD ESP as shown in Fig. 5(b). Clearly, the particle reentrainment occurred for the conventional ESP and dominated with large particle size greater than 2000 nm as time elapsed or particles deposited on the collection plate which was relevant from the reentrainment theory by the conventional ESP as shown from Fig. 5(a). On the other hand, the collection efficiency of average of 80% was achieved for the EHD ESP for particle size of 2000nm or greater and particle reentrainment was clearly suppressed.

Fig. 6 shows the particles-size dependent collection efficiency between vertically and horizontally oriented EHD

ESP by SMPS using a 435cc diesel engine. The collection efficiency for the horizontally oriented EHD ESP was superior for particle size of 20~500nm except 100-120nm range. This may be related to electrohydrodynamic (EHD)

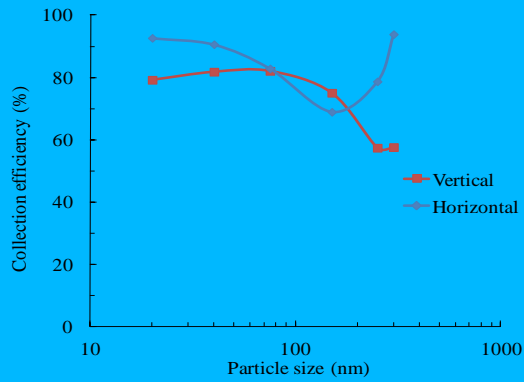


Fig. 6. Comparison between vertically and horizontally oriented electrodes EHD ESP by SMPS using 435cc diesel engine

more than 90% was achieved for the entire particle size range in 300-5000nm. However, the particle size of 300-500nm range was significantly improved in comparison with the vertically oriented EHD ESP as shown in Fig. 7 but the

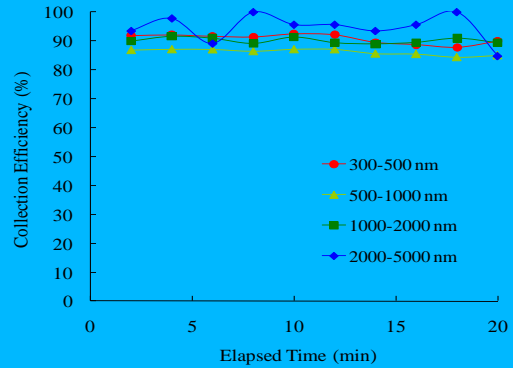


Fig. 8. Particle size-dependent number density collection efficiency measured by PC for horizontally oriented electrode

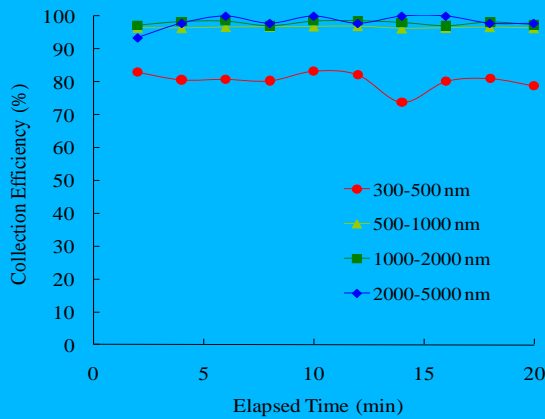


Fig. 7. Particle size-dependent number density collection efficiency measured by PC for vertically oriented EHD ESP using 400cc diesel engine

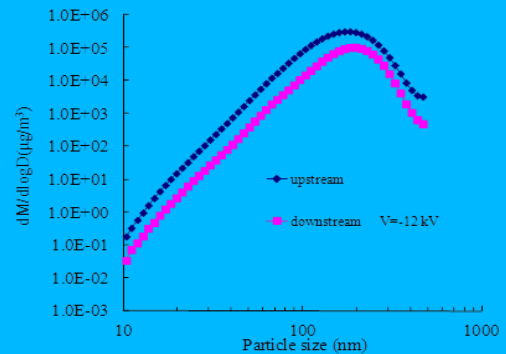


Fig. 9(a). Particle size-dependent mass collection efficiency measured by SMPS for vertically oriented EHD ESP

effects on collection efficiency, which will be discussed later. Note that experiments were conducted 5 times for SMPS and 10 times for PC measurements, respectively to achieve the confidence levels of the collection efficiency.

On the other hand, particle size-dependent number density collection efficiency measured by PC for the vertically oriented EHD ESP was shown in Fig. 7. More than 95% collection efficiency was achieved for particle-size range between 300-5000nm except particle size of 300-500nm, which the average collection efficiency of 80% was achieved. This was attributed to field and diffusion mixed particle changing ranges, resulting in lower collection efficiency based on classical charging theory [1].

Fig. 8 shows particle size-dependent number density collection efficiency measured by PC for the horizontally oriented electrode EHD ESP. The collection efficiency of

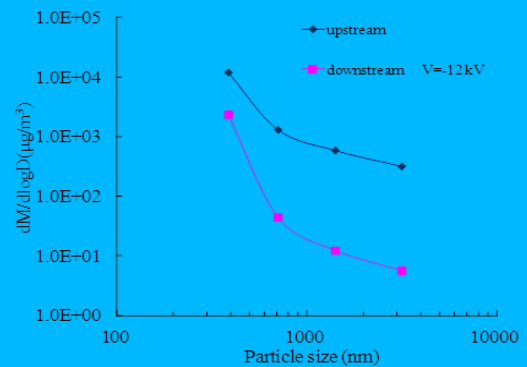


Fig. 9(b). Particle size-dependent mass collection efficiency measured by PC for vertically oriented EHD ESP

overall collection efficiency for 300-500nm showed somewhat lower for the horizontally oriented EHD ESP.

Fig. 9(a) shows particle size-dependent mass collection efficiency measured by SMPS for vertically oriented electrode. The mass base collection efficiency for the particle size range of 20-500nm was 71.8% Fig. 9(b) shows the mass base collection efficiency which was 83.0 %. The overall collection efficiency was 73.1%.

Fig. 10(a) shows particle size-dependent mass collection efficiency measured by SMPS for horizontally oriented EHD ESP. The mass base collection efficiency for the particle size range of 20-500nm was 73.8% Fig. 10(b) shows the mass base collection efficiency which was 90.5 %. The overall collection efficiency was 76.0%, indicating in the overall mass collection was dominated by the small particle size range owing to high number density.

Based on the collection efficiency for vertically and horizontally oriented electrode configuration on the EHD ESP, the horizontally oriented EHD ESP performed better especially the particle size of 300-500nm range.

In order to understand the electrohydrodynamics of the EHD ESP, the current density distribution was measured at -10, -11, and -12kV and the current maximum current density was 30, 56, and 91  $\mu\text{A}$ , respectively, since ionic wind is proportional to the square root of the current density. Fig. 11(a) and Fig. 11(b) show the normalized current density distribution for vertically and horizontally oriented electrode EHD ESPs, respectively. There are two peaks: one was the highest current density at the upstream pocket corner and the

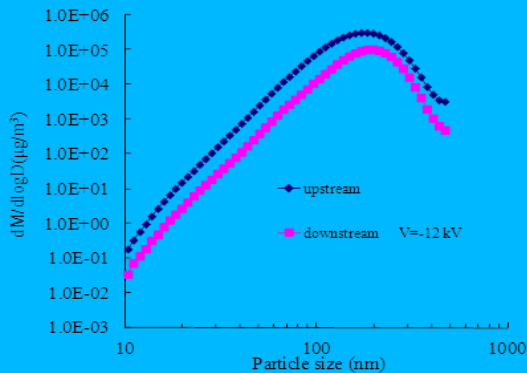


Fig. 10(a). Particle size-dependent mass collection efficiency measured by SMPS for horizontally oriented EHD ESP

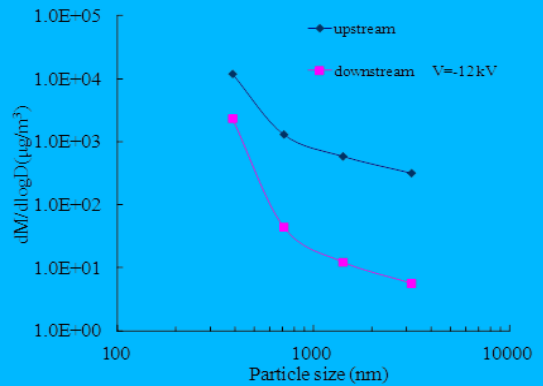


Fig. 10(b). Particle size-dependent number mass collection efficiency measured by PC for horizontally oriented EHD ESP

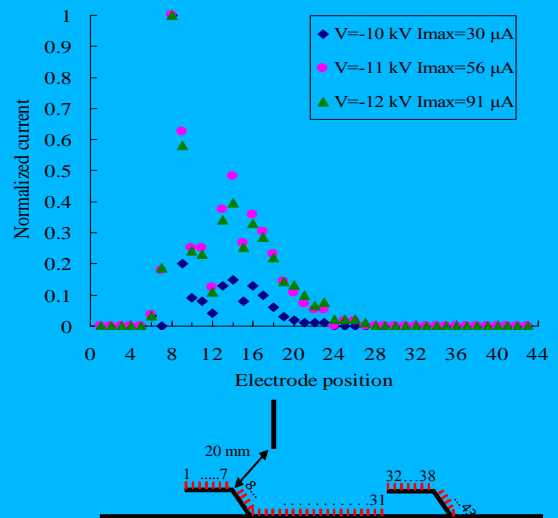


Fig. 11(a) Normalized current density distribution for vertically oriented electrode EHD ESP

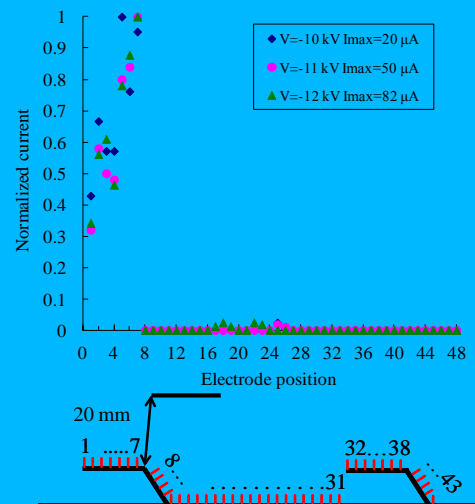


Fig. 11(b) Normalized current density distribution for horizontally oriented electrode EHD ESP

other was just beneath the saw electrode of about 50% of the maximum current density as shown in Fig. 11(a). The EHD becomes complicated. On the other hand, the horizontally oriented electrode has the maximum current density at the upstream side of the pocket alone. To understand the electrohydrodynamics of the EHD ESP, Schlieren technique, which makes temperature gradient visible, was employed to visualize the average flow in the inter electrode space of the EHD ESP.

Fig. 12(a) shows the streamlines for the vertical oriented EHD ESP. The flow is moving from left to right. Since it is difficult to identify the flow, the schematic flow diagram was shown in Fig. 12(b). The average gas stream started to move towards the electrode and reflected back to the collection plate after passing the electrode, which results in a large recirculation cell behind the pocket zone. Another recirculation was generated inside of the pocket but this recirculation was weakened by the holes backside of the pockets by releasing the buildup pressure.



Fig. 12(a). Streamlines for the vertical oriented EHD ESP using the Schlieren photograph for vertically oriented EHD ESP

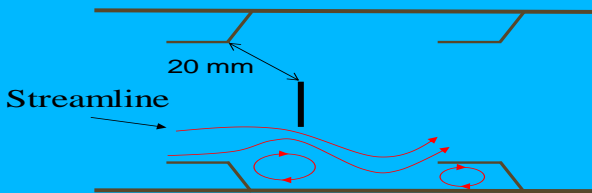


Fig. 12(b) Schematic flow diagram for Schlieren photograph for vertically oriented EHD ESP

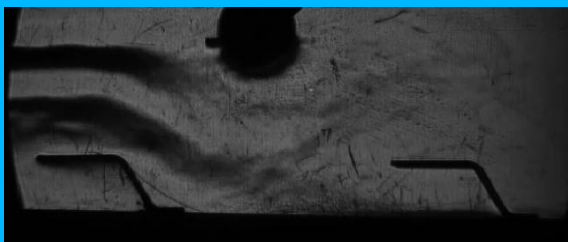


Fig. 13(a). Streamlines for the vertical oriented EHD ESP using the Schlieren photograph for horizontally oriented EHD ESP

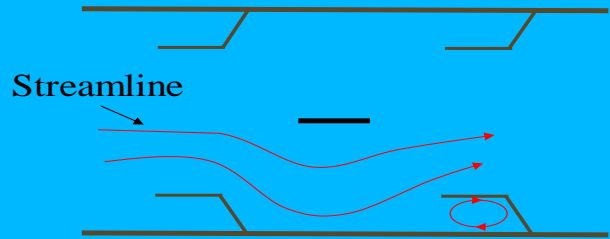


Fig. 13 (b). Schematic flow diagram for Schlieren photograph for horizontally oriented EHD ESP

Fig. 13(a) shows the streamlines for the horizontally oriented EHD ESP using the Schlieren photograph. The schematic flow diagram was shown in Fig. 13(b). The recirculation generated behind the upstream side of the pocket for the case of vertically oriented EHD ESP was disappeared and more smooth streamlines were observed, which trapped particles within the recirculation zone behind the upstream side of the pocket may be transported into the backside of the pocket region more effectively. This was a plausible explanation for enhancement of the collection efficiency for horizontally oriented EHD ESP. Another reason was due to reduced gas velocity in the vicinity of the electrode location. The EHD ESP particularly horizontally oriented electrode EHD ESP showed significant reduction of reentrainment over the conventional ESPs even with different diesel engines used. However, we are still looking for the optimum design to minimize the reentrainment for the EHD ESP by transporting the charged particle into the pocket zone or low electric field zones effectively and minimizing the electric field exposed area even with the increased gas velocity in the range of 10 m/s. The EHD ESP has high potential especially for highly concentrated marine diesel engine emission control.

#### IV. SUMMARY

The collection of low resistive particles generated from diesel engine was investigated using vertically and horizontally oriented EHD ESP. The conventional ESP showed good collection efficiency for particle size less than 300 nm where adhesion force was dominated over electrostatic repulsion force but showed severe reentrainment for the particle size greater than 1,000 nm. The vertically oriented EHD ESP showed a good collection efficiency for the whole particle size ranging 20-5000nm except 300-500nm. On the other hand, the horizontally oriented EHD ESP showed an excellent collection efficiency for the entire particle size range investigated and the particle reentrainment

totally suppressed for larger particles. The EHD ESP has high potential especially for highly concentrated marine diesel engine emission control.

#### ACKNOWLEDGMENT

Authors wish to thank you for support by Grant-in-Aid for Scientific Research (B) of the Japanese Society for the Promotion of Science, the Ocean Policy Research Foundation (OPRF), and the Nippon Foundation derived from Motorboat Racing.

#### REFERENCES

- [1] "Handbook of Electrostatics" Ed. S. Masuda, Ohm Press, Institute of Electrostatics Japan
- [2] J.D. Bassett, K. Akutsu, S. and Masuda, "A Preliminary Study of Re-entrainment in an Electrostatic Precipitator," *Journal of Electrostatics*, Vol. 3, 1977, pp. 311-257.
- [3] R. M. Felder, E. Arce-Medina, "Radiotracer Measurement of Local Desposition Profiles, Friction Reentrainment and Impaction Reentrainment in an Electrostatic Precipitator," *AICHE Journal*, Vol. 31, No. 1, 1985, pp. 82-89.
- [4] T. Takahashi, Y. Kawada, A. Zukeran, Y. Ehara, and T. Ito, "Inhibitory Effect fo Coating Elctrodes with Dielectric Sheet on Re-entrainment in Electrostatic Precipitator," *Journal of Aerosol Science*, Vol. 29, Suppl. 1, 1998, pp.s481-s82.
- [5] A. Zukeran, Y. Ikeda, Y. Ehara, M. Matsuyama, T. Ito, T. Takahashi, H. Kawakami, and T. Takamatsu, "Two-Stage Type Electrostatic Precipitator Re-entrainment Phenomena under Diesel Flue gases," *IEEE Trans. Ind. Applications*, Vol. 35, No. 2, 1999, pp. 346-351.
- [6] A. Zukeran, Y. Ikeda, Y. Ehara, T. Ito, T. Takahashi, H. Kawakami, and T. Takamatsu, "Agglomeration of Particles by ac Corona Discharge," *EEJ*, Vol. 130, No. 1, 2000, pp. 30-37.
- [7] K. Yasumoto, A. Zukeran, Y. Takagi, Y. Ehara, T. Takahashi, and T. Ito, "Suppression of Particle Deposition onto Downstream Wall in n AC Electrostatic Precipitator with Neutralization," *Int. Journal of Environment and Waste Management*, Vol. 2 NOs 4/5, 2008, pp.399-411.
- [8] T. Yamamoto, T. Abe, T. Mimura, Y. Ito, N. Otsuka, Y. Ehara, and A. Zukeran, "Electrodynamically-Assisted Electrostatic Precipitator for Collection of Low Resisitive Diesel Particulates," *IEEE Transactions on Industry Applications* Vol. 46, No. 4, July Aug. 2010, pp. 1606-1612.
- [9] T. Yamamoto, T. Abe, T. Mimura, Y. Otsuka, Y. Ehara, and A. Zukeran, "Electrohydrodynamically Assisted Electrostatic Precipitator for the Collection of Low Resistive Dust," *IEEE Transactions on Industry Applications*, Vol. 45, No. 6, Nov./Dec. 2009, pp. 2178-2184.
- [10] T. Yamamoto, T. Mimura, S. Asada, and Y. Ehara, "Diesel Emission Control using EHD-Assisted Electrostatic Precipitator Combined with Plasma Processes," *International Journal of Plasma Environmental Science and Technology*, Vol. 5, No. 1, 2011, pp. 31-36.
- [11] A.D. Zimon, Adhesion of Dust and Powder, Plenum Press, New York, London 1969.
- [12] B. J. Sung, A. Aly, S. H. Lee, K. Takashima, S. Katsura, and A. Mizuno, "Fine Particles Collection Using an Electrostatic Precipitator Equipped with an Electrostatic Flocking Filter as the Collecting Electrode," *Plasma Processes and Polymers*, vol. 3, pp. 661-667, 2006.
- [13] T. Yamamoto, and H.R. Velkoff, "Electrohydrodynamics in an Electrostatic Precipitator." *J. of Fluid Mechanics*, Vol. 108, 1981, pp. 1-18.
- [14] H.Y. Wen and G. Gasper, "On the Kinetics of Particle Reentrainment from Surface," *J. Aerosol Science*, Vol. 20, 1989, pp. 483-498.
- [15] M.W. Reeks, J. Red, and D. Hall,"On the Resuspension of Small Particles by a Turbulent Flow," *J. Physics D, Applied Physics*, Vol. 21, 1988, pp. 574-589.
- [16] M.M.R. Williams, "An Exact Solution of the Reek-Hall Resuspension Equation for Particulate Flow," *J. Aerosol Science*, Vol. 23(1), 1992, pp. 1-10.
- [17] T. Yamamoto, M. Okuda, and M. Okubo, "Three Dimensional Ionic Wind and Electrohydrodynamics of Tuft/Point Corona Electrostatic Precipitators," *IEEE Transactions on Industry Applications*, Vo. 39, No. 6, Nov/Dec 2003, pp. 1603-1607.
- [18] H. Fujishima, Y. Morita, M. Okubo, and T. Yamamoto, "Numerical Simulation of Three-Dimensional Electrohydrodynamics of Spiked-Electrode Electrostatic Precipitators," *IEEE Transactions on Dielectric and Electrical Insulation*, Vo. 13, No. 1, Feb. 2006, pp. 160-167.